

Abrupt coupling between strongly dissimilar waveguides with 100% transmission

André Kurs,^{1,*} John D. Joannopoulos,¹
Marin Soljačić,¹ and Steven G. Johnson²

¹*Department of Physics, Massachusetts Institute of Technology, Massachusetts 02139, USA*

²*Department of Mathematics, Massachusetts Institute of Technology, Massachusetts 02139, USA*

[*akurs@alum.mit.edu](mailto:akurs@alum.mit.edu)

Abstract: We present numerical experiments showing how coupled-mode theory can be systematically applied to join very dissimilar photonic crystal waveguides with 100% transmission. Our approach relies on appropriately tuning the coupling of the evanescent tail of a cavity mode to each waveguide. The transition region between the waveguides may be as short as a few lattice spacings. Moreover, this technique only requires varying a small number of parameters (two for each waveguide in our example) and the tuning to each waveguide may be done separately, greatly simplifying the computations involved.

© 2011 Optical Society of America

OCIS codes: (130.3120) Integrated optics devices; (130.2790) Guided waves.

References and links

1. E. Yablonovitch, "Inhibited spontaneous emission in solid-state physics and electronics," *Phys. Rev. Lett.* **58**, 2059–2062 (1987).
2. S. John, "Strong localization of photons in certain disordered dielectric superlattices," *Phys. Rev. Lett.* **58**, 2486–2489 (1987).
3. J. D. Joannopoulos, S. G. Johnson, J. N. Winn, and R. D. Meade, *Photonic Crystals: Molding the Flow of Light*, 2nd ed. (Princeton University Press, 2008).
4. Y. Xu, R. K. Lee, and A. Yariv, "Propagation and second-harmonic generation of electromagnetic waves in a coupled-resonator optical waveguide," *J. Opt. Soc. Am. B* **17**, 387–400 (2000).
5. M. Soljačić, S. G. Johnson, S. Fan, M. Ibanescu, E. Ippen, and J. D. Joannopoulos, "Photonic-crystal slow-light enhancement of nonlinear phase sensitivity," *J. Opt. Soc. Am. B* **19**, 2052–2059 (2002).
6. T. Baba, "Slow light in photonic crystals," *Nat. Photonics* **2**, 465–473 (2008).
7. S. P. Anderson, A. R. Shroff, and P. M. Fauchet, "Slow light with photonic crystals for on-chip optical interconnects," *Adv. Opt. Technol.* **2008**, 293531 (2008).
8. M. L. Povinelli, S. G. Johnson, and J. D. Joannopoulos, "Slow-light, band-edge waveguides for tunable time delays," *Opt. Express* **13**, 7145–7159 (2005).
9. N. Moll and G.-L. Bona, "Comparison of three-dimensional photonic crystal slab waveguides with two-dimensional photonic crystal waveguides: efficient butt coupling in these photonic crystal waveguides," *J. Appl. Phys.* **93**, 4986–4991 (2003).
10. P. Sanchis, P. Bienstman, B. Luyssaert, R. Baets, and J. Marti, "Analysis of butt coupling in photonic crystals," *IEEE J. Quantum Electron.* **40**, 541–550 (2004).
11. E. Miyai and S. Noda, "Structural dependence of coupling between a two-dimensional photonic crystal waveguide and a wire waveguide," *J. Opt. Soc. Am. B* **21**, 67–72 (2004).
12. Y. A. Vlasov and S. J. McNab, "Coupling into the slow light mode in slab-type photonic crystal waveguides," *Opt. Lett.* **31**, 50–52 (2006).
13. T. P. White, L. C. Botten, C. M. de Sterke, K. B. Dossou, and R. C. McPhedran, "Efficient slow-light coupling in a photonic crystal waveguide without transition region," *Opt. Lett.* **33**, 2644–2646 (2008).

14. P. Velha, J. P. Hugonin, and P. Lalanne, "Compact and efficient injection of light into band-edge slow-modes," *Opt. Express* **15**, 6102–6112 (2007).
15. C. M. de Sterke, J. Walker, K. B. Dossou, and L. C. Botten, "Efficient slow light coupling into photonic crystals," *Opt. Express* **15**, 10984–10990 (2007).
16. S. Boscolo, C. Conti, M. Midrio, and C. G. Someda, "Numerical analysis of propagation and impedance matching in 2-D photonic crystal waveguides with finite length," *J. Lightwave Technol.* **20**, 304–310 (2002).
17. S. Boscolo, M. Midrio, and T. F. Krauss, "Y junctions in photonic crystal channel waveguides: high transmission and impedance matching," *Opt. Lett.* **27**, 1001–1003 (2002).
18. A. Mekis and J. D. Joannopoulos, "Tapered couplers for efficient interfacing between dielectric and photonic crystal waveguides," *J. Lightwave Technol.* **19**, 861–865 (2001).
19. T. D. Happ, M. Kamp, and A. Forchel, "Photonic crystal tapers for ultracompact mode conversion," *Opt. Lett.* **26**, 1102–1104 (2001).
20. S. G. Johnson, P. Bienstman, M. A. Skorobogatiy, M. Ibanescu, E. Lidorikis, and J. D. Joannopoulos, "Adiabatic theorem and continuous coupled-mode theory for efficient taper transitions in photonic crystals," *Phys. Rev. E* **66**, 066608 (2002).
21. P. Sanchis, J. Garcia, A. Martinez, F. Cuesta, A. Griol, and J. Marti, "Analysis of adiabatic coupling between photonic crystal single-line-defect and coupled-resonator optical waveguides," *Opt. Lett.* **28**, 1903–1905 (2003).
22. P. Sanchis, J. Martí, W. Bogaerts, P. Dumon, D. Van Thourhout, and R. Baets, "Experimental results on adiabatic coupling into soi photonic crystal coupled-cavity waveguides," *IEEE Photon. Technol. Lett.* **17**, 1199–1201 (2005).
23. K. Dossou, L. C. Botten, C. M. de Sterke, R. C. McPhedran, A. A. Asatryan, S. Chen, and J. Brnovic, "Efficient couplers for photonic crystal waveguides," *Opt. Commun.* **265**, 207–219 (2006).
24. P. Pottier, M. Gnan, and R. M. De La Rue, "Efficient coupling into slow-light photonic crystal channel guides using photonic crystal tapers," *Opt. Express* **15**, 6569–6575 (2007).
25. J. P. Hugonin, P. Lalanne, T. P. White, and T. F. Krauss, "Coupling into slow-mode photonic crystal waveguides," *Opt. Lett.* **32**, 2638–2640 (2007).
26. A. Mutapcic, S. Boyd, A. Farjadpour, S. G. Johnson, and Y. Avniel, "Robust design of slow-light tapers in periodic waveguides," *Eng. Optimiz.* **41**, 365–384 (2009).
27. H. A. Haus, *Waves and Fields in Optoelectronics* (Prentice-Hall, 1984).
28. A. F. Oskooi, D. Roundy, M. Ibanescu, P. Bermel, J. D. Joannopoulos, and S. G. Johnson, "MEEP: a flexible free-software package for electromagnetic simulations by the FDTD method," *Comput. Phys. Commun.* **181**, 687–702 (2010).
29. A. Yariv, Y. Xu, R. K. Lee, and A. Scherer, "Coupled-resonator optical waveguide: a proposal and analysis," *Opt. Lett.* **24**, 711–713 (1999).
30. D. O'Brien, M. D. Settle, T. Karle, A. Michaeli, M. Salib, and T. F. Krauss, "Coupled photonic crystal heterostructure nanocavities," *Opt. Express* **15**, 1228–1233 (2007).
31. S. G. Johnson and J. D. Joannopoulos, "Block-iterative frequency-domain methods for Maxwell's equations in a planewave basis," *Opt. Express* **8**, 173–190 (2001).
32. S. Fan, S. G. Johnson, J. D. Joannopoulos, C. Manolatu, and H. A. Haus, "Waveguide branches in photonic crystals," *J. Opt. Soc. Am. B* **18**, 162–165 (2001).
33. A. Taflove and S. C. Hagness, *Computational Electrodynamics: The Finite-Difference Time-Domain Method* (Artech, 2000).
34. A. Farjadpour, D. Roundy, A. Rodriguez, M. Ibanescu, P. Bermel, J. D. Joannopoulos, and S. G. Johnson, "Improving accuracy by subpixel smoothing in the finite-difference time domain," *Opt. Lett.* **31**, 2972–2974 (2006).
35. V. A. Mandelshtam and H. S. Taylor, "Harmonic inversion of time signals and its applications," *J. Chem. Phys.* **107**, 6756–6769 (1997).
36. S. Noda, M. Fujita, and T. Asano, "Spontaneous-emission control by photonic crystals and nanocavities," *Nat. Photonics* **1**, 449–458 (2007).
37. A. F. Oskooi, L. Zhang, Y. Avniel, and S. G. Johnson, "The failure of perfectly matched layers, and towards their redemption by adiabatic absorbers," *Opt. Express* **16**, 11376–11392 (2008).
38. A. Mekis, J. C. Chen, I. Kurland, S. Fan, P. R. Villeneuve, and J. D. Joannopoulos, "High transmission through sharp bends in photonic crystal waveguides," *Phys. Rev. Lett.* **77**, 3787–3790 (1996).
39. S. Mahmoodian, R. C. McPhedran, C. M. de Sterke, K. B. Dossou, C. G. Poulton, and L. C. Botten, "Single and coupled degenerate defect modes in two-dimensional photonic crystal band gaps," *Phys. Rev. A* **79**, 013814 (2009).
40. S. G. Johnson, C. Manolatu, S. Fan, P. R. Villeneuve, and J. D. Joannopoulos, "Elimination of cross talk in waveguide intersections," *Opt. Lett.* **23**, 1855–1857 (1998).
41. B. E. Little, S. T. Chu, H. A. Haus, J. Foresi, and J.-P. Laine, "Microring resonator channel dropping filters," *J. Lightwave Technol.* **15**, 998–1005 (1997).

1. Introduction

In this paper, we provide a general prescription for, and specific examples of, how abrupt interfaces between a photonic crystal cavity and two waveguides may be tailored so that 100% transmission between the waveguides is achieved. Photonic crystals enable an extraordinary degree of control over the propagation of light and a rich variety of phenomena [1–3]. Connecting different photonic crystal devices in an efficient manner is therefore critical to enabling complex integrated photonic devices. Slow-light waveguides, for example, have greatly enhanced sensitivity to nonlinear effects, thus facilitating the design of compact electro-optical devices [4–7], but coupling to them can be particularly challenging [8]. For a variety of applications, our proposal may present an alternative to approaches such as butt-coupling [9, 10], mode-field matching [11–13], anti-reflection coating-like injectors [14, 15], optical stub tuners [16, 17], and tapered transitions between waveguides [18–26]. The approach explored in this paper exploits the property known as “ Q -matching” in the abstract framework of coupled-mode theory [27], which provides an accurate phenomenological approximation to the full physics, provided that the coupling between any two distinct structures is sufficiently weak. A Q -matching structure typically only needs to be a few lattice spacings long: little more than a single period of the slow-light coupled-cavity waveguide (shorter than typical adiabatic tapers). Although resonant

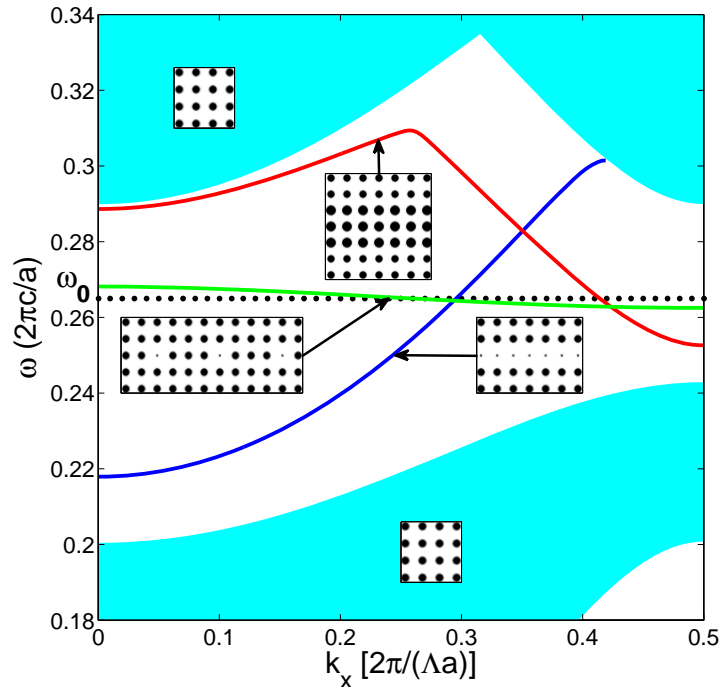


Fig. 1. Projected band diagram along the $\Gamma-X$ direction for TM modes in a square lattice of rods of radius $a/4$ (shaded region) and band structures for a singly-wide line defect, triply-wide line defect, and coupled-cavity waveguide (identified by their dielectric profile). The defect radii are, respectively, $a/12$, $0.325a$, and $a/12$. The constant Λ (x -axis of the figure) is 4 for the CCW and 1 for the other structures, due to the longer primitive cell ($4a$) of the former, along the direction of the propagation.

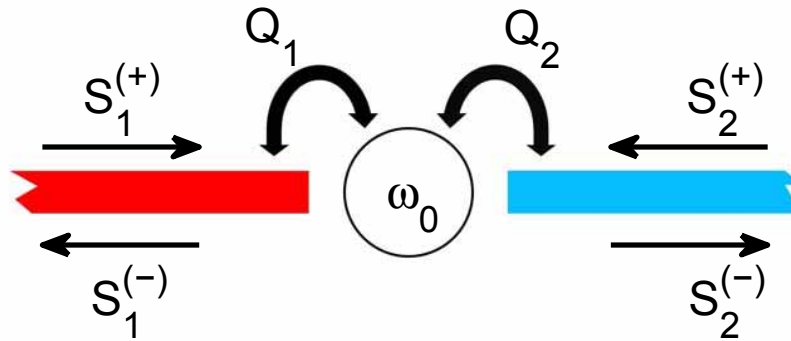


Fig. 2. Graphical representation of a coupled-mode theory treatment of two waveguides (red and blue strips) coupled by means of a cavity tuned to resonate at the angular frequency ω_0 and couple to each waveguide with quality factors Q_1 and Q_2 . The direct coupling between the two waveguides is neglected. 100% transmission occurs at the frequency ω_0 when $Q_1 = Q_2$.

phenomena are necessarily narrow bandwidth, in our case the resonance bandwidth is comparable to that of the slow-light waveguide itself, so the Q -matching strategy does not worsen the intrinsic sensitivity of the problem to perturbations. Furthermore, the reliance of our design on only a small number of tuned parameters makes post-fabrication tuning a possibility to compensate for imperfections. We begin by introducing three different photonic crystal waveguides within a square lattice of silicon rods in silica. Next, we show how coupled-mode theory may be applied to split the overall transmission problem into substantially more tractable parts by allowing each waveguide to be separately matched to a single-defect cavity. Finally, once all three waveguide-cavity structures are properly tuned, we check the validity of the tuning procedure and demonstrate 100% transmission by fully simulating the transmission for all combinations of two distinct waveguides. Both the tuning and verification are done via full simulations of Maxwell's equations with no approximation except for the discretization [28].

2. Exemplar waveguides

For concreteness, we consider three different kinds of waveguides formed by introducing linear defects into a two-dimensional square lattice (with lattice constant a) of rods of radius $r = a/4$ and permittivity $\epsilon_{\text{high}} = 12.25$ embedded in a dielectric material with $\epsilon_{\text{low}} = 2.25$. (These values of the dielectric constants approximately correspond to those for silicon and fused silica in the near infrared, respectively.) The first waveguide is a standard linear defect waveguide formed by substituting one column of rods in the original square lattice by a column of rods with smaller radius $a/12$. The second waveguide is a triply-wide linear defect wherein three adjacent columns of the square lattice are replaced with rods of larger radius $0.325a$, and the last waveguide is a coupled-cavity waveguide [29, 30] (CCW) in which every fourth rod along a column is replaced with a rod of radius $a/12$. The permittivity of the defect rods is the same as that of the original rods (ϵ_{high}) in all three waveguides. Figure 1 shows the dielectric function profiles for the three waveguides analyzed as well as the relevant TM bands (computed by

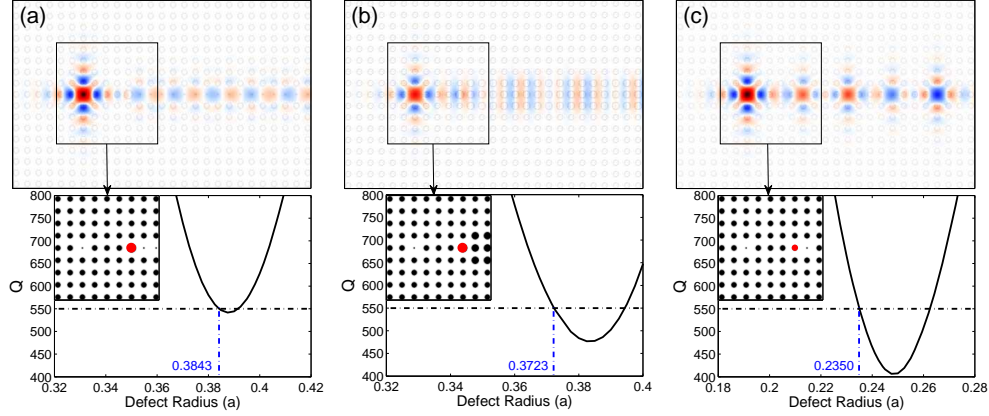


Fig. 3. Results of a finite-difference time-domain (FDTD) simulation of a cavity resonant at $\omega_0 = 0.265 \times (2\pi c/a)$ decaying into a singly-wide line defect waveguide (a), a triply-wide line defect waveguide (b), and a slow-light coupled-cavity waveguide (c). The top panels show the z component (parallel to the rods) of the electric field. The insets show the dielectric profile of the area indicated. The lower panels show the dependence of the cavity Q on the defect radius of the rod closest to the waveguide (insets, in red). The latter are tuned so that the Q of the cavity is 550 in each case. The values of the defect radii indicated in blue are used in the full simulations of the coupled waveguides.

preconditioned conjugate-gradient minimization of the block Rayleigh quotient in a planewave basis [31]) and the projected band diagram for TM modes of the square lattice of rods. Since the CCW has its inflection point (and thus zero group velocity dispersion) at the center-gap frequency $\omega_0 = 0.265 \times (2\pi c/a)$, we take ω_0 as the target frequency for which the transmission is to be maximized.

3. Design and tuning of the coupling cavity

We now turn to the design of a compact resonant cavity to mediate the transmission between any two waveguides. If we impose the requirement that the resonant structure be weakly coupled to each waveguide and that the direct coupling between waveguides be in turn negligible compared to their interaction with the cavity, then the key phenomenon of interest is well described by the temporal coupled-mode theory equations [3, 27]

$$\frac{dA}{dt} = -i\omega_0 \left(1 - i \sum_m \frac{1}{2Q_m} \right) A + \sum_m \sqrt{\frac{\omega_0}{Q_m}} S_m^{(+)}, \quad (1)$$

$$S_m^{(-)} = -S_m^{(+)} + \sqrt{\frac{\omega_0}{Q_m}} A, \quad (2)$$

where $A(t)$ denotes the complex amplitude of the cavity's excitation and is normalized such that the energy associated with the cavity is $|A|^2$, ω_0 is the resonant frequency of the cavity, the index m denotes the different waveguides, and Q_m is the quality factor of the cavity's decay into waveguide m . $S_m^{(+)}$ and $S_m^{(-)}$ represent, respectively, the complex amplitudes of the waveguide modes going towards and away from the cavity, and are normalized such that the power flowing in each mode is given by $|S_m^{(\pm)}|^2$. A schematic of the coupled-mode theory of the particular

system considered in this paper (one cavity coupled to two waveguides) is shown in Fig. 2. The transmission $T(\omega) = \left| S_2^{(-)} / S_1^{(+)} \right|^2$ for this setup is readily found by solving Eqs. (1) and (2) when $S_1^{(+)}$ is set to a constant and $S_2^{(+)} = 0$:

$$T(\omega) = \frac{\omega_0^2 / (Q_1 Q_2)}{(\omega - \omega_0)^2 + \left(\frac{1}{2Q_1} + \frac{1}{2Q_2} \right)^2 \omega_0^2}, \quad (3)$$

which equals unity (100% transmission) at $\omega = \omega_0$ if $Q_1 = Q_2$ (a property often referred to as the Q -matching condition [32]) and has a bandwidth set by the quality factors. It follows that we can approach the problem of coupling two dissimilar waveguides with a three-step process: 1) design a cavity that resonates at the desired frequency, 2) separately model the cavity in conjunction with a single waveguide and tune each cavity-waveguide interface so as to achieve a target coupling Q , and 3) as a check (if desired), simulate the full system with two waveguides and the cavity. For each step, we performed simulations using the finite-difference time-domain method [33] (FDTD), implemented in a freely available software package [28], with a resolution of 16 pixels per lattice spacing and subpixel smoothing of the dielectric function [34] in order to more accurately model the finer features of the structure. In the first two steps, we used the filter-diagonalization method [35] to extract the resonant frequency and Q of the cavity and the waveguide. Note that because the discretization of the system is the same across all FDTD simulations, the resonant frequency and Q values extracted from the decay computations (which may differ from the exact result because of the finite resolution) are directly applicable to the simulation of the transmission. Thus, regardless of errors introduced by the discretization, the transmission spectrum should peak at 100% in the transmission calculation provided that the coupling Q 's of the cavities extracted from the decay computations match, as predicted by coupled-mode theory arguments. Similar considerations may be used to correct for perturbations introduced in fabrication, which can be circumvented as long as the Q 's of the fabricated cavity can be retuned and matched to the same value. Although we have assumed that the system is lossless, it is straightforward to modify the coupled-mode theory treatment to account for losses due to, e.g., radiation or absorption [3] (which would then reduce the peak of the transmission from 100%). Since we presently work with coupling $Q < 10^3$ between the cavity and the waveguides and photonic crystal cavities with loss Q 's in excess of 10^6 have been demonstrated experimentally [36], our assumption that the cavity is lossless (and consequently enables 100% transmission between waveguides) should be a reasonable approximation for appropriately designed experimental systems.

4. Discussion

We found that a point-defect formed by replacing one lattice rod with a rod of same dielectric constant ϵ_{high} and radius $0.1095a$ had a resonant frequency within 0.05% of the target $\omega_0 = 0.265 \times (2\pi c/a)$. For tuning the Q of the cavity coupled to each waveguide (Fig. 3), we varied two parameters: the number of lattice periods separating the cavity from the waveguide (a discrete parameter) and the radius of the rod closest to the waveguide. We found that at a separation of four lattice spacings, all three systems had local minima in the vicinity of $Q = 550$, which we chose as our target. (Note that it may often be desirable to tune Q to a value close to a local minimum, as this is where the slope of Q as a function of the continuous parameter is smallest, thereby improving the robustness of the tuning with respect to perturbations in the tuning parameter due to imperfections in the fabrication.) After finding the optimal tuning parameters for each system, we verified that all combinations of dissimilar waveguides coupled by means of the cavity and properly tuned intervening structure exhibited 100% transmission

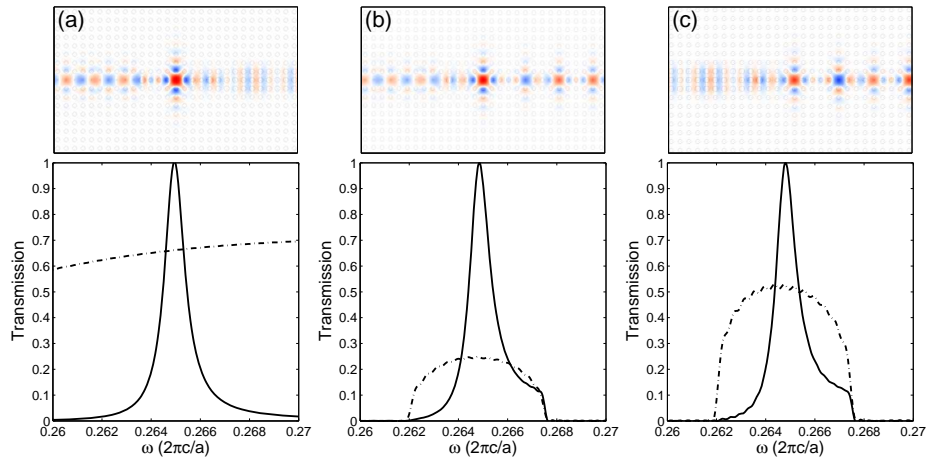


Fig. 4. FDTD simulations showing the z component of the electric field (top panels) and the transmission spectrum of a singly-wide line defect waveguide coupling to triply-wide waveguide (a), a singly-wide waveguide coupling to a CCW (b), and a triply-wide waveguide coupling to a CCW (c). Each system is tuned to the points indicated (in blue) in Fig. 3 and exhibits 100% transmission near $\omega_0 = 0.265 \times (2\pi c/a)$. For reference, the transmission spectra of the corresponding butt-coupled geometries are shown as dash-dotted lines.

at $\omega = \omega_0$ by a direct FDTD calculation of the transmission between waveguides (Fig. 4). This simulation involves driving the leftmost waveguide with a spatially localized and temporally gaussian excitation and letting the resulting electromagnetic pulse propagate through the structure while recording the values of the fields through a flux plane intersecting the rightmost waveguide. The transmission spectrum at a given frequency may then be calculated by Fourier-transforming the fields at the flux plane, computing the associated Poynting vector, integrating it over the flux plane, and normalizing the result to the power spectrum of the excitation. Although we terminate the waveguides with absorbing boundaries (pseudo perfectly matched layers, pPMLs [37]), we have further minimized the effect of possible numerical artifacts due to the pulse being reflected at the pPMLs by tuning the running time of the simulation and the length of the waveguides so that the electromagnetic pulse substantially propagates through the flux plane exactly once [38]. Because of the increased size of the computational volume and longer timescales, these transmission simulations are considerably more numerically intensive than those shown in Fig. 3 (a single transmission computation typically taking more time to complete than a full decay parameter search such as those shown in the lower panels of Fig. 3) and it would be far less practical to use them directly to search for the appropriate tuning parameters, especially for three-dimensional systems. Nevertheless, they bear out the prediction of 100% transmission from the coupled-mode theory combined with a set of much simpler cavity decay simulations. Note that the bandwidth of the CCW is comparable to the $Q = 550$ between the cavity and each waveguide, and the transmission spectra to the CCW [Figs. 4(b) and 4(c)] deviate from the Lorentzian shape predicted by Eq. (3) as they approach the band-edges of the CCW (beyond which the transmission drops to zero as there are no propagating CCW modes to couple to). Also shown (as dash-dotted lines) in Fig. 4 are the transmission spectra of the corresponding butt-coupled structures, where the terminal defect rods of the two coupled waveguides are in neighboring periods of the underlying photonic crystal lattice. One can see that, although the butt-coupled transmission spectra have broader bandwidths than the

Q -matched results, they do not achieve 100% transmission over the frequency range of interest. Although the butt-coupled transmission could be improved by tweaking the interface between the two waveguides, this would generally require solving a mode-field matching problem in its own right, and any delicate cancelation of the reflected wave would itself be a narrow-bandwidth resonant effect.

5. Applicability to other waveguide junctions

Note that due to the symmetry of the square lattice of the underlying photonic crystal, the junctions shown in Fig. 3 could have just as well been used in a 90° bend coupling one waveguide to another. Indeed, the prescription outlined in this paper may be applied directly to any system comprising two single-mode waveguides and a single-mode cavity that fulfills the condition of sufficiently weak coupling required for a coupled-mode theory treatment. Provided these simple conditions are met, Q -matching could be used, for instance, to couple modes of very different symmetry and polarization (e.g. TE to TM or TEM_{01} to HE_{11}) and is not limited to photonic crystals. Note that even if the cavity mode happens to be doubly degenerate [39], such symmetry-induced degeneracies will only support one mode that couples to the waveguide mode in waveguides with mirror symmetry, yielding effectively single-mode behavior [40]. Finally, it should be possible to obtain broader transmission bandwidths by extending this technique to (non-degenerate) multi-mode cavities [41].

Acknowledgments

We thank Mike Watts for helpful discussions. This work was supported by the MRSEC Program of the NSF under Award No. DMR-0819762 and by the U.S.A.R.O. through the ISN under Contract No. W911NF-07-D-0004.